ELSEVIER

Journal of Molecular Structure (Theochem) 423 (1998) 153–159

THEO CHEM

Binding between the CD4 receptor and polysulfonated azo-dyes. An exploratory theoretical study on action-mechanism[1]

Zoltán Sze'kely[a,b,*], Péter Fábián[c], Ladislaus L. Torday[d], Christopher J. Michejda[a], Adorján Aszalós[e]

[a]*Molecular Aspects of Drug Design, MSL, ABL-Basic Research Program, NCI-Frederick Cancer Research and Development Center, Frederick, MD 21702-1201, USA*

[b]*Department of Medical Chemistry, Albert Szent-Györgyi Medical University, Szeged, Hungary*

[c]*Institute of Biochemistry, Agricultural Biotechnology Center, Gödöllő, Hungary*

[d]*Department of Pharmacology, Albert Szent-Györgyi Medical University, Szeged, Hungary*

[e]*Division of Research and Testing, CDER, Food and Drug Administration, Washington DC, USA*

Abstract

The antiviral mechanism of action of the polysulfonated azo-dyes is discussed in this paper. Crucial to the antiviral activity of these dyes is the inhibition of the HIV entry into the host cell. This is a result of the covering strategic areas of the CD4 viral receptor surface. A consistent, mainly electrostatic, interaction model has been established to explain the mode of inhibition activity of Direct Red 79 and Direct Yellow 50. The basis of the model is a dynamic distance matrix of the most important positively charged amino acid side chains within the CD4, which might serve as an electrostatic docking site for the negatively charged sulfonate groups of the azo-dyes. Beside the intrinsic value of interpreting the biological effect, this model might serve as a useful tool for a rational drug design. Published by Elsevier Science B.V.

Keywords: HIV entry; CD4; gp120; Antiviral drug; Docking

1. Introduction

During the past decade, various compounds were under scrutiny for development as effective anti-AIDS drugs. In addition to the well known enzyme inhibitors, the investigation of viral entry [1] is an interesting field of AIDS research.

Several polysulfonated aromatic molecules are known to be active as antiviral agents [2–4]. According to the literature, two main action mechanisms for their antiviral activity have been proposed: (1) enzyme inhibition (against reverse transcriptase [3,4] and integrase [5]), (ii) HIV entry inhibition [3].

This paper focuses on the second point. The molecular recognition between the HIV-1 envelope glycoprotein (gp120) and its receptor (CD4) is a well defined process both from the biological and structural points of view [1,6,7]. Several papers have been published in connection with molecular modeling of this field [8–10]. As it is apparent in Fig. 1, the crucial part of the interaction consists of three

* Corresponding author.

[1] By acceptance of this article, the publisher or recipient acknowledges the right of the U.S. Government and its agents and contractors to retain a nonexclusive royalty-free licence in and to any copyright covering the article.

PII S0166-1280(97)00363-1

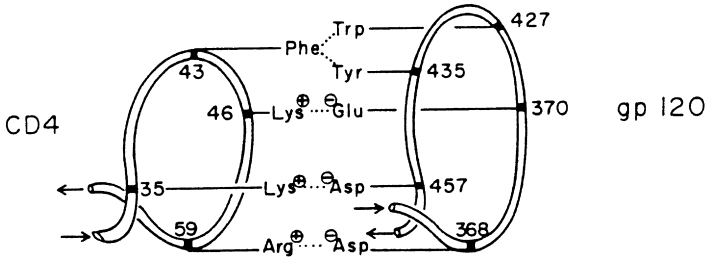

Fig. 1. A schematic representation of the CD4–gp120 recognition process. Final stage: electrostatic attachment and aromatic locking in. The pairing scheme shown for the charged moieties is purely arbitrary.

salt-bridges (positive side chains on the CD4 surface, Lys^{35}, Lys^{46} and Arg^{59}, combined with the negative side chains on the gp120 surface, Asp^{368}, Glu^{370} and Asp^{457}). Finally, during this process, this complex becomes more compact through an aromatic stacking interaction (Phe^{43} of CD4 and Trp^{427}, Tyr^{435} of gp120).

From the several examples of previously investigated polysulfonated dyes, we have selected two compounds for molecular modeling, due to their structural similarity and highly different biological activity.

The structures of the selected dyes, Direct Red 79 (DR79) and Direct Yellow 50 (DY50), are shown in Fig. 2.

2. Methods

2.1. Flow cytometric anti-Leu3a-FITC binding assay

The biological assay was a competitive binding measurement between αLeu3a monoclonal antibody and dye molecules to the CD4 surface, because previous work indicated that the antibody and the dye have very similar binding sites on CD4. This binding site is located at the D1 domain of the CD4. The HIV-1 envelope glycoprotein (gp120) binds to the same region of the CD4 surface. The inhibition activities of the dyes of 3 μg ml^{-1} concentration were represented as a decrease in fluorescence of the fluorescein-labeled gp120 bound to the cell surfaces [11].

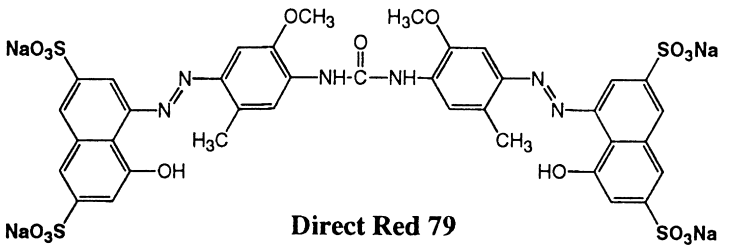

Direct Red 79

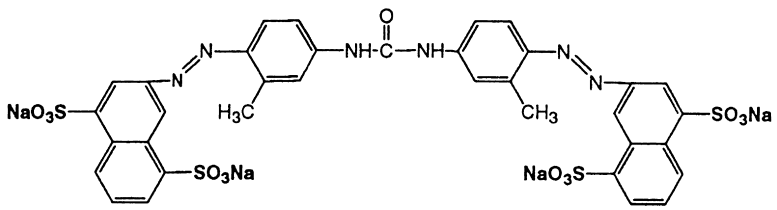

Direct Yellow 50

Fig. 2. Structural formulas of DY50 and DR79.

2.2. Molecular modeling techniques

The original three-dimensional coordinate file of the CD4 D1 and D2 domains was obtained from the Protein Data Bank. This coordinate set [12] represents the structure of the CD4 (1–182 residues) at a resolution of 2.2 Å. The SYBYL program package (Tripos Inc.) was utilized for the computations. After an accurate energy minimalization (10^{-3} kcal Å^{-1} mol^{-1} convergence criteria was used), a long term dynamical simulation (MD) was performed. The main parameters of the MD calculations were 12 ps heating period, 162 ps total simulation time. During the 102 ps of the analysis, the conformations were archived in 340 cases. In this time period the average temperature was 293.9 K (std. dev. 2.73 K) and the average energy was –1754.41 kcal mol^{-1} (std. dev. 64.25 kcal mol^{-1}).

3. Results and discussion

Of the two selected azo-dyes, namely the Direct Red 79 (DR79) and Direct Yellow 50 (DY50), the former has been shown [11] to bind strongly to the CD4 surface while the latter showed only marginal affinity. Yet both azo-dyes contain disulfonated naphthalene ring moieties. It is clear from the examination of the dye structures (Fig. 2), that the two $-SO_3^-$ moieties are arranged differently in the two molecules. In the biologically non-active DY50, the two $-SO_3^-$ groups are on opposite sides of the naphthalene rings, while in the biologically active DR79 the two $-SO_3^-$ functionalities are on the same side (Fig. 2).

The S···S distance ($d_{S\cdots S}$), which measures the spatial separation of the two $-SO_3^-$ moieties, was used as a geometrical descriptor. The great advantage of ($d_{S\cdots S}$) is that it is a conformationally invariant

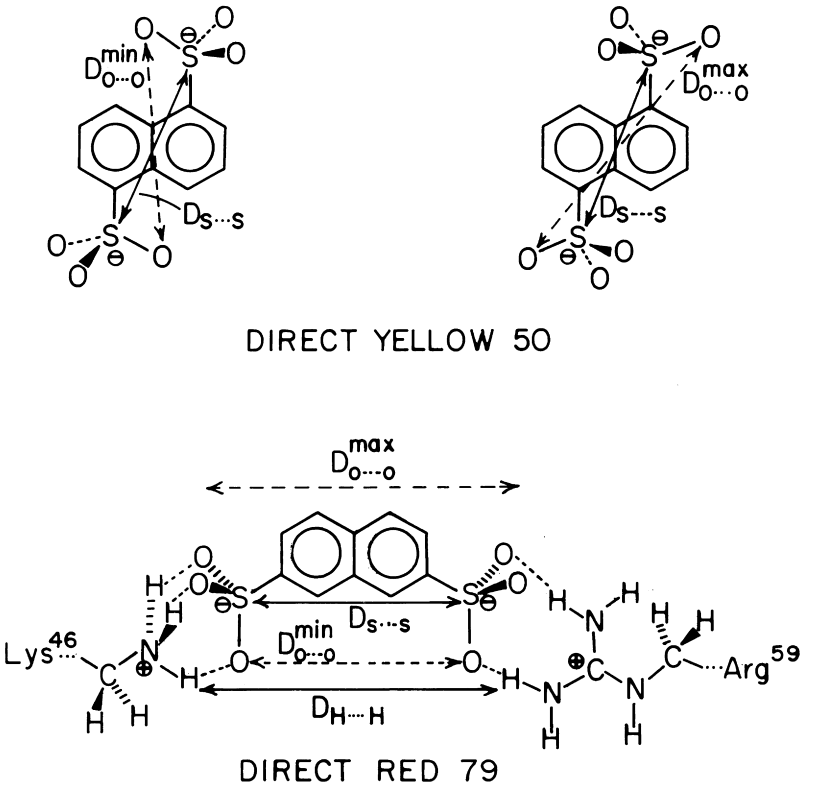

Fig. 3. Critical distances in two isometric disulfonated naphthalenes as they mimic azo-dyes: DY50 (upper part) and DR79 (lower part). An example of distance between hydrogen atoms of Lys^{46} and Arg^{50} side chains.

Table 1
Biological activities and S···S as well as O···O distances of the polysulfonated dye molecules. The biological activities are represented as inhibition abilities of the CD4–αLeu3a monoclonal antibody interaction, on the basis of fluorescence intensity of CD4-bound, fluorescein-labeled αLeu3a without dye treatment

Dye	Biological activity (remaining fluorescence %)	Geometry/Å	
		S···S distance	O···O distance
DR79	8	8.13	7.32–10.12
DY50	100	6.74	7.35–8.89

quantity while $d_{O\cdots O}$ is a conformationally dependent quantity varying between $d_{(O\cdots O)min}$ and $d_{(O\cdots O)max}$. From Fig. 3 we may conclude by inspection the following relationships:

Direct Yellow 50 : $d_{(O\cdots O)max} > d_{(O\cdots O)min} > d_{(S\cdots S)}$

Direct Red 79 : $d_{(O\cdots O)max} > d_{(S\cdots S)} > d_{(O\cdots O)min}$

However, it is also clear from Fig. 3 that even the shortest H···H distance ($d_{(H\cdots H)min}$) between the positively charged amino acid side chains is greater than any of the above geometrical descriptors:

$d_{(H\cdots H)min} > d_{(O\cdots O)max}$

Fig. 3 shows this explicitly for DR79.

The experimentally determined biological activities of the two azo-dyes, as well as their optimized $d_{S\cdots S}$ values are summarized in Table 1. Interestingly, DY50 has a shorter S···S distance than DR79; but the $d_{S\cdots S}$ value is much better suited for complexation in the case of DR79. The $d_{H\cdots H}$ values computed by MD simulations are given in Table 2.

If the positively charged side chain-ends of Lys[46] and Arg[59] approach the naphthalene moiety in such a way that the $\cdots CH_2{-}NH_3^+$ bond is in alignment with one of the $\cdots C{-}SO_3^-$ bonds and the $\cdots NH{-}C(NH_2)_2^+$ bond is in alignment with the other $\cdots C{-}SO_3^-$ bond, then the number of hydrogen bonds, and therefore the stabilization energy, are maximized. This corresponds to a planar approach as illustrated for DR79 in Fig. 3 and for DY50 in Fig. 4. If, however, a perpendicular approach is operative in the complexation process, shown as one of the two limiting alternatives in Fig. 4, then the number of hydrogen bonds and therefore the associated stabilization energy will be less than the previous maximum.

It is not surprising that DY50 does not form a stable complex with CD4 while DR79 does, since the location of the two –SO– groups in the former allows only the weak, perpendicular complexation to occur. The $d_{S\cdots S}$ is too short for DY50 and the value then is much better suited for complexation in the case of DR79.

Table 3 shows the computed energy components

Table 2
Dynamic distance matrix for the side chain terminal N–H protons of lysine[46] and arginine[59] [a]

	Arg[59]				
	H-atoms	1867	1868	1869	1870
Lys[46]	1766	9.25–12.49 (**11.19**, *0.62*)	9.91–14.11 (**12.45**, *0.71*)	11.16–15.90 (**14.15**, *0.89*)	11.85–15.69 (**14.00**), *0.81*)
	1767	9.38–12.47 (**11.21**, *0.60*)	10.25–13.84 (**12.30**, *0.69*)	11.16–15.85 (**14.20**, *0.86*)	11.76–15.48 (**13.91**, *0.79*)
	1768	8.01–11.25 (**9.97**, *0.62*)	9.03–12.69 (**11.18**, *0.70*)	9.82–14.75 (**13.13**, *0.87*)	10.50–14.34 (**12.86**, *0.80*)
	Average	8.01–12.49 (**10.8**)	9.03–14.11 (**12.0**)	9.82–15.90 (**13.8**)	10.50–15.69 (**13.6**)

[a] Distances are measured in Ångstroms. The means are given in bold numbers and the standard deviations are numbers in italics; both of them are shown in brackets. The numbering of the H-atoms was derived from the automatic numbering system of the SYBYL program.

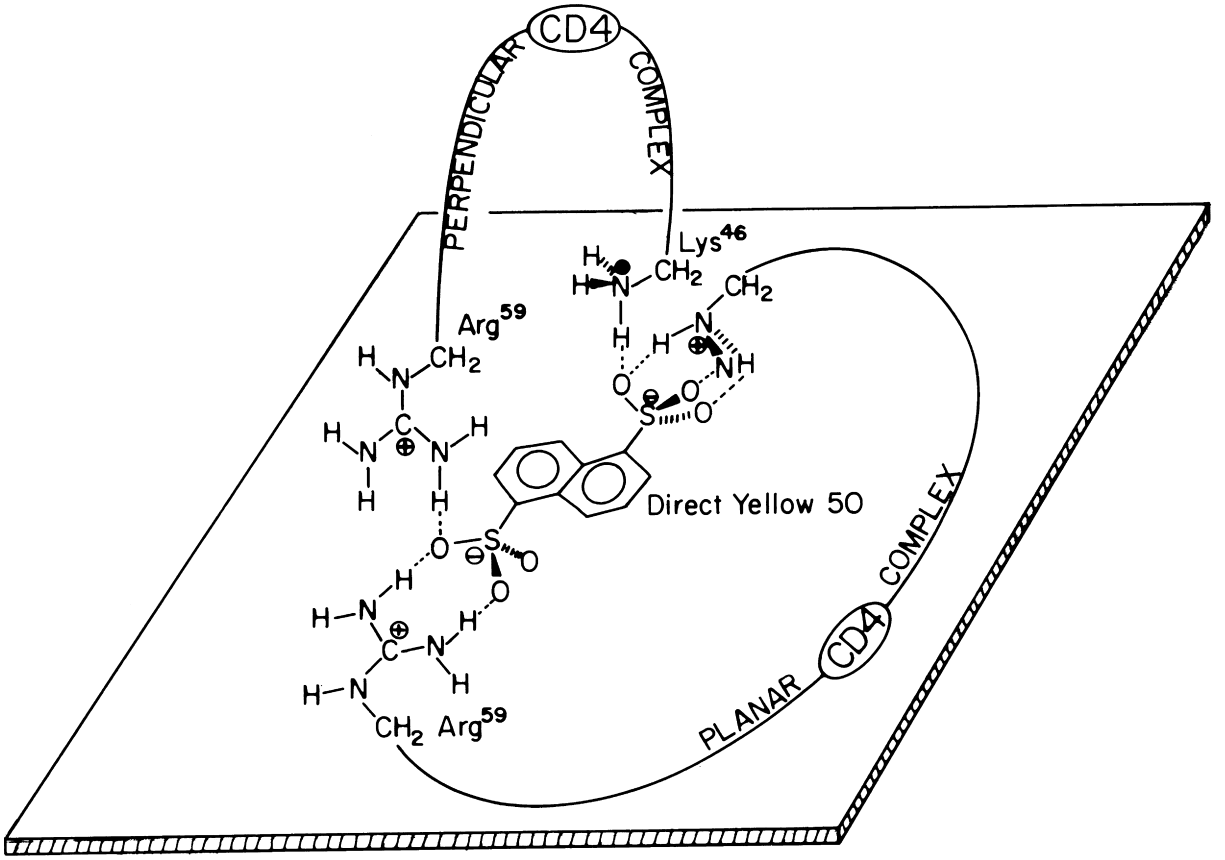

Fig. 4. Coplanar and perpendicular limiting alternatives for complexation between CD4 and DY50.

and their sums for CD4, DR79, DY50, and for their complexes. The last line of the table lists the complexation energies.

$$CD4 + DR79 \rightarrow [CD4\cdots DR79]$$

$$CD4 + DY50 \rightarrow [CD4\cdots DY50]$$

It is clear from Table 3 that [CD4···DR79] is more stable than [CD4···DY50] by -41.48 kcal mol^{-1}. This excess stability originates almost exclusively from the electrostatic contributions, as might be expected from the interaction of the negatively charged azo-dyes and the positively charged CD4. This energy difference can be seen to be accounted for by the -45.84 kcal mol^{-1} ''electrostatic'' term in Table 3, entry 8. (The intermolecular electrostatic interaction is included in this term.)

4. Conclusions

To explain the highly different binding activities of Direct Red 79 and Direct Yellow 50 to the CD4 receptor, a clear structure–activity relationship is suggested. Due to the computational difficulties of docking (i.e. the determination of the starting geometries as well as the ''driving'' of the docking procedure, etc.) a dynamic distance matrix (DDM) has been established for the most important amino acid side chains of the CD4 before the calculation of the docking energy. This new feature has been proven to be a powerful tool to estimate the dynamical docking behavior of the CD4 receptor surface moieties. Based on the DDM and the S···S distances of the two sulfonate moieties in the axo dyes, the DR79 proved to be the better binding molecule to the CD4 receptor surface.

Table 3
Docking energies and energy terms of the model compounds for CD4···DR79 as well as CD4···DY50 complex formation. The energy values were obtained after minimization in all cases (all of them are given in kcal mol^{-1})

	Energy	CD4	DR79	DY50	CD4 + DR79	[CD4···DR79]	CD4 + DY50	[CD4···DY50]
1	Bond stretching	48.413	0.179	0.533	48.592	48.078	48.946	47.187
2	Angle bending	242.155	1.020	2.159	243.175	253.136	244.314	251.320
3	Torsional	261.637	5.916	6.439	267.553	267.535	268.076	270.237
4	Out-of-plane bending	8.641	0.074	0.005	8.715	8.549	0.8.646	9.225
	Bonded internal subtotal (1 + 2 + 3 + 4)	560.846	7.189	9.136	568.035	577.298	569.982	577.969
5	1–4 van der Waals	128.725	0.866	0.651	129.591	139.349	129.376	131.066
6	van der Waals	–616.919	–1.325	–0.184	–618.244	–623.339	–617.103	–627.140
7	1–4 Electrostatic	1951.418	–14.548	17.625	1936.870	1935.213	1969.043	1968.393
	1–4 Electrostatic docking	–	–	–	0.000	–0.657	0.000	–0.650
8	Electrostatic	–3632.254	19.113	22.522	–3613.141	–3943.583	–3609.732	–3894.321
	Electrostatic docking	–	–	–	0.000	–330.442	0.000	–284.589
	Relative electrostatic docking	–	–	–	–	0.000	–	45.834
	Non-bonded internal subtotal (5 + 6 + 7 + 8)	–2169.030	4.106	40.614	–2164.924	–2501.369	–2128.416	–2422.002
	Total	–1608.184	11.295	49.750	–1596.889	–1924.071	–1558.434	–1844.033
	Docking energy	–	–	–	0.00	–327.182	0.00	–285.599
	Relative docking energy	–	–	–	–	0.00	–	41.583

In the other series of calculations, the energies obtained for the CD4 dye complexes, as well as for their components, had led us to formulate similar conclusions, namely, better complexation occurs between DR79 and CD4 (i.e. the complexation energy between the DR79 and CD4 was lower than that of DY50–CD4 complex formation). This molecular modeling approach may be useful for the interpretation of the antiviral activities of the various polysulfonated compounds.

Acknowledgements

Research sponsored in part by the National Cancer Institute, DHHS, under contract with ABL. The contents of this publication do not necessarily reflect the views or policies of the Department of Health and Human Services, nor does mention of trade names, commercial products, or organizations imply endorsement by the US Government. The financial support of the Hungarian Science Foundation (OTKA F13060) as well as a grant for computational equipment provided by the Higher Educational Development Foundation (FEFA HU-525) is gratefully acknowledged. Two of the authors (L.L. Torday and Z. Székely) are grateful for Eötvös Fellowships granted by the National Scholarship Board of the Ministry of Culture and Education (Hungary) as well as for a fellowship provided by the World Bank (W15085). The MD calculations were partially made at the Agricultural Biotechnology Centre, Gödöllö, Hungary. Thanks are due to Professors B. Penke and J. Molnár (A. Szent-Györgyi Medical University, Szeged, Hungary) as well as A. Perczel (Loránd Eötvös University, Budapest, Hungary) for helpful discussions. Special thanks are due to Professor I. G. Csizmadia (University of Toronto, Toronto, Canada) for his helpful advice.

References

[1] J.P. Moore, R.W. Sweet, Perspectives in Drug Design (Suppl. of Computer-Aided Drug Design), 1 (1993) 235–250.
[2] H. Mitsuya, M. Popovic, R. Yarchoan, S. Matsushita, R.C. Gallo, S. Broder, Science 226 (1984) 172–174.
[3] D.J. Clanton, R.A. Moran, J.B. McMahon, O.S. Weislow, R.W.Buckheit Jr., M.G. Hollingshead, V. Ciminale, B.K. Felber, G.N. Pavlakis, J.P. Bader, J. AIDS 5 (1992) 771–781.
[4] D. Rideout, R. Schinazi, C.D. Pauza, K. Lovelane, L.-C. Chiang, T. Calogeropoulou, M. McCarthy, J.H. Elder, J. Cell. Biochem. 51 (1993) 446–457.

[5] S. Carteau, J.F. Mouscadet, H. Goulanouic, F. Subra, C. Auclair, Arch. Biochem. Biophys. 305 (1993) 606–610.
[6] S.C. Harrison, J. Wang, Y. Yan, T. Garrett, J. Liu, U. Moebius, E. Reinherz, Cold Spring Harbor Symposia on Quantitative Biology 57 (1992) 541–548.
[7] S.C. Harrison, Acc. Chem. Res. 26 (1993) 449–453.
[8] Z. Székely, A. Perczel, B. Penke, J. Molnár, J. Mol. Struct. (Theochem) 286 (8) (1993) 165–182.
[9] L.M. Ptaszek, S. Vijayakumar, G. Ravishanker, D.L. Beveridge, Biopolymers 34 (1994) 1145–1153.
[10] Z. Székely, Z. Kónya, A. Becskei, W.P.D. Goldring, A. Perczel, B. Penke, J. Molnár, C.J. Michejda, A. Aszalós, I.G. Csizmadia, J. Mol. Struct. (Theochem) 36 (1997) 159–186.
[11] J.L. Weaver, P.S. Pine, R. Anand, S. Bell, A. Aszalós, Antiviral Chem. Chemother. 3 (1993) 147–151.
[12] T.P.J. Garrett, J. Wang, Y. Yan, J. Liu, S.C. Harrison, J. Mol. Biol. 234 (1993) 763–778.